|| Volume 7 || Issue 8 || October 2023 || ISSN (Online) 2456-0774
INTERNATIONAL JOURNAL OF ADVANCE SCIENTIFIC RESEARCH
AND ENGINEERING TRENDS

"Earthquake Analysis and Response of Intake -outlet Towers"

[1]Mr. Kapil M. Sindhikar, [2]Dr. Nagesh Shelke
M.E Civil (Structural Engineering)

[1]PG Student, Department of Civil Engineering, Dr. D.Y. Patil College of Engineering & Technology, Lohegaon, Charholi(BK)
[2]Professor, Department of Civil Engineering,, Dr. D.Y. Patil College of Engineering & Technology, Lohegaon, Charholi(BK)
India

Abstract— *in this paper, the results of a analysis for the seismic response of a hydropower station intake tower in step-like ground based on artificial boundary theory topography are presented. The topography finite element model was established to verify the correctness of the proposed method of viscous elasticity boundary by considering inconsistent reflective surface. After applying the method to an intake tower, the acceleration of bedrock was determined using the seismic inversion method, and the equivalent load of each node was afterwards estimated. Following is a list of the five different models that were established as follows: massless foundation, consistent input viscous elasticity boundary, inconsistent input viscous elasticity boundary, and whether set contact. After comparing displacement and stress, the results show that the proposed method with contact was the least disruptive. It is possible to draw the conclusion that the intake tower is in a state of overall stability since the base plate of the intake tower and the foundation were in a state of close adhesion during the entire process of the earthquake, both the sides and the rear side of the intake tower did not experience any disengagement phenomena from rock, and so on. Key Words: Fly over, design parameters, bending moment shear force, post processing, Staad Pro Connect.*

Keywords: Tower, Intake –Outlet Tower, Staad Pro Connect, Earthquake

INTRODUCTION

Intake towers ensure water control project seismic safety as the project progresses. L-shaped rock terrain uses bank-tower intakes. The intake tower-mountain relationship impacts inlet deformation and stress.
Seismic properties and loading determine engineering seismic analysis. Inversion of bedrock seismic data from ground acceleration increases seismic load realism.
Dynamic analysis considers the superstructure's elastic foundation effect. Radiation dampening impacts foundations narrowly. Stable, efficient, and ubiquitous, local artificial boundaries partially decouple time and space. Many researchers found the viscoelastic boundary to be exact, stable, and easy to design in finite element software as a local artificial barrier.
Scholars' three-dimensional viscoelastic artificial barrier intake tower dynamic analysis was accurate and applicable. Three-dimensional viscoelastic barrier; flat terrain is best. The project's high-rock bank-tower intake is steep.

Study the basin topography viscoelastic boundary and solve seismic wave motion of stepped topography utilizing virtual symmetric substructure. Dynamic amplification rises with free face displacement amplitudes and slope gradient. Symmetrical studies

virtual processed the high and low side into 2D equally high boundary to overcome the steep topography viscoelastic boundary inconsistent input problem. But the back-tower intake position at 3D L-shape terrain, before and after the tower, has a high mutation level, not a gradient slope, and dynamic analysis requires three-directional seismic input, so it cannot change into two-dimensional difficulties. Thus, these methods cannot resolve the issue.
Different backfill concrete heights and forms affect the intake tower because the link between the tower, backfill concrete, and rock is not completely solidified. studies the model of set contact between the intake tower and the surrounding rock, showing that the tower's tensile stress can be released and the stress level reduced, near to the actual condition. These investigations assume a massless foundation without foundation radiation damping.
The intake tower's viscoelastic boundary with high rock is realized in this work. The method is tested numerically. Calculated models with varied boundary conditions are discussed. Engineering recommendations conclude.
Based on earlier viscoelastic boundary research, developed the method for abrupt step topography and used it to dynamically analyze an intake tower in a hydropower station.
Tower displacement and stress under massless foundation and contact conditions are compared. Bank-tower intake with homogenous foundation can be analysed dynamically using this method.
When the ground surface has obvious hyper mutation, viscoelastic artificial boundary should be used to calculate sub-regional node load, enlarged at the highly abrupt volley surface and greater than the incident and reflected superposition value.
Consider the intake tower-rock-foundation interface. An earthquake's closed, separated, or sliding tower-rock state. Set contact parts can release tensile stress and lessen acceleration along the tower height, closer to reality. In practical engineering, bank-tower intake is a popular water inlet that backs to the mountain for stability but cuts the mountain slope during construction, creating a steep landscape. This study shows that step topography must be considered, and suitable viscoelastic boundary setting and load input are made.
Design, modelling, environmental analysis, and direct operation are the primary steps of any nuclear power unit (NPU). At the above stages, the installation concept is evaluated and its parameters are accurately estimated because building such an installation is very expensive.

Planning and production management difficulties involve many factors that change with external conditions.

Simulation, which provides qualitative and quantitative estimations of managed decision outcomes, is one of the most promising activities. Simulation methods dominate management theory and operations research in industrial companies and organizations.
They help analyze functioning to improve production and management processes and coordinate and regulate all subsystems.

Problem Statement

"Design considerations and to design the parametric Study in nuclear tower such as parameters and also to know the process of prefabrication of various structural elements".

Aim

"Analysis of the Earthquake and the Reaction of the Intake and Outlet Towers because the joints between the structural elements of a structure will not create a structural system until much later, structural concerns for stability and safety must be made at each stage of the process."

Objectives

- The main objective of designing of power intake outlet towers as nuclear power plant
- Design and analyze the Power plant using software Staad pro Connect
- We devise a technique to do the performance analysis of safety critical and control systems and to estimate performance based risk factor
- To Analyze Non-functional requirements plays a critical role in designing variety of applications domain ranges from safety-critical systems to simple gaming applications

Methodology

- Study for literature review survey
- To study the construction techniques of method we have gone through various research papers, books, and some field works
- Building design using Static Linear Analysis.
- Building plan using AutoCAD
- Dynamic analysis using Staad Pro Connect software
- Study of prefabricated structure and all parameters
- Analysis result
- Result and discussion
- Conclusion

Design and Analysis

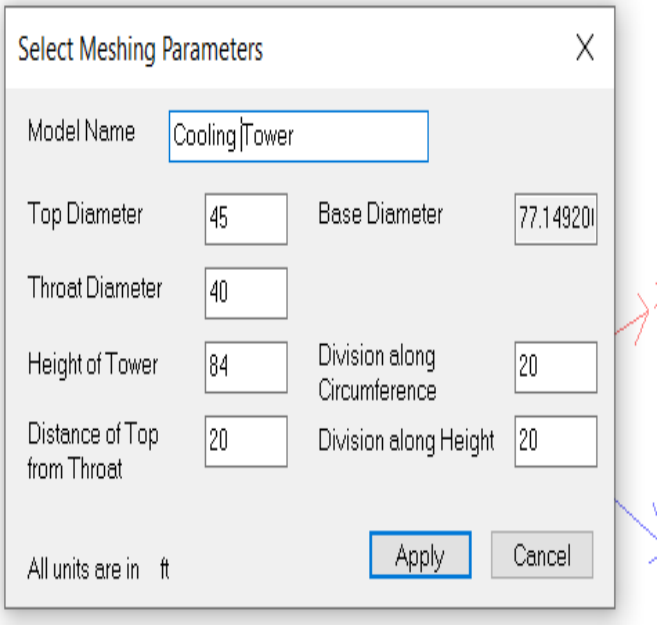

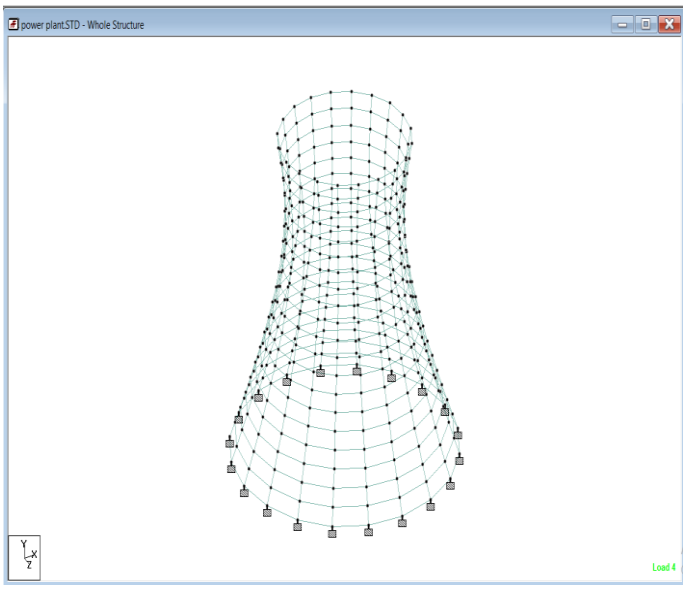

Design and Modelling

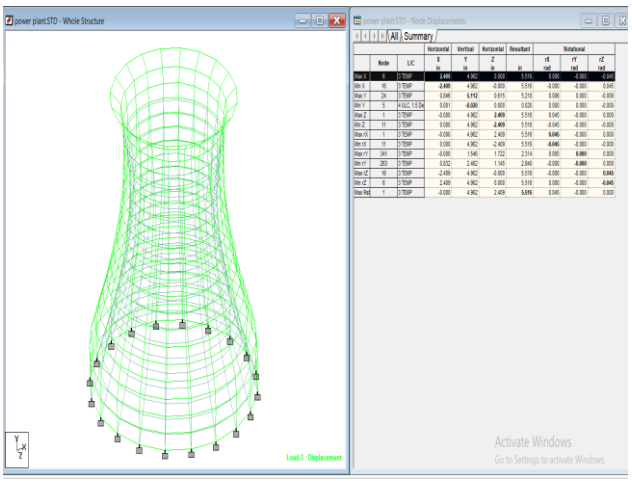

Figure1.2: Displacement Due to Temperature Loading

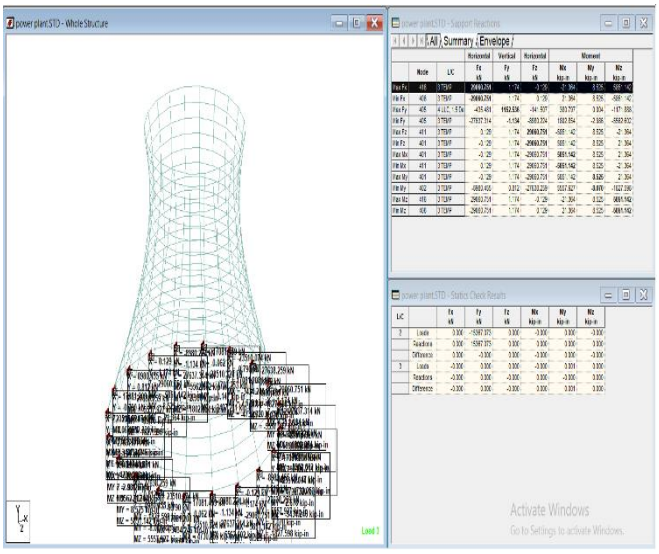

Figure1.3: Maximum Base Reaction

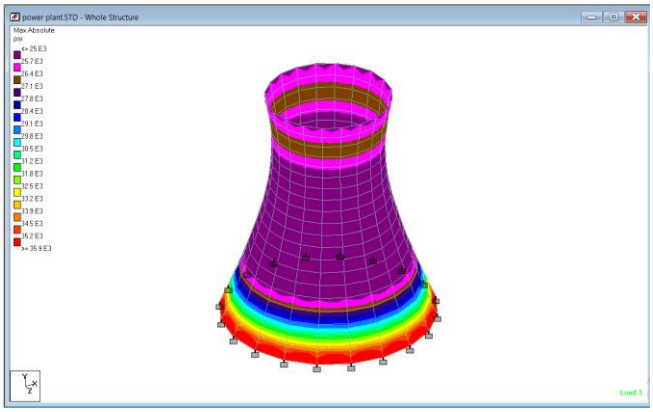

Figure1.4: Plate stresses due to temp loading

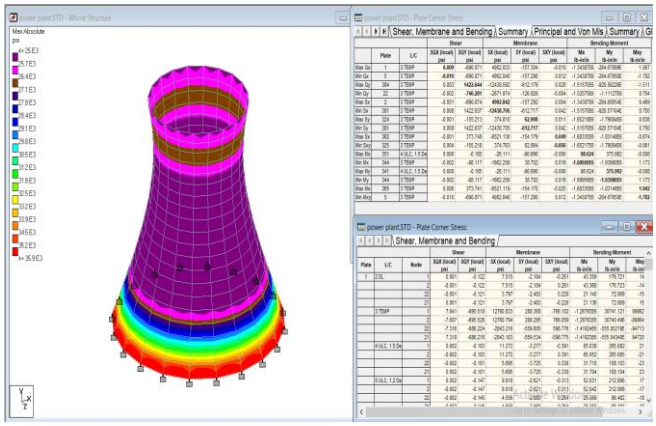

Figure1.5: SHEAR FORCE AND BMD RESULT TABLE

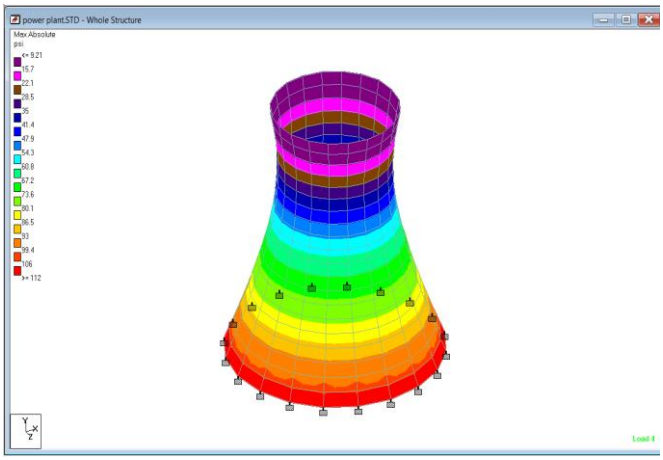

Figure1.6: STRESSES DUE TO DEAD LOAD

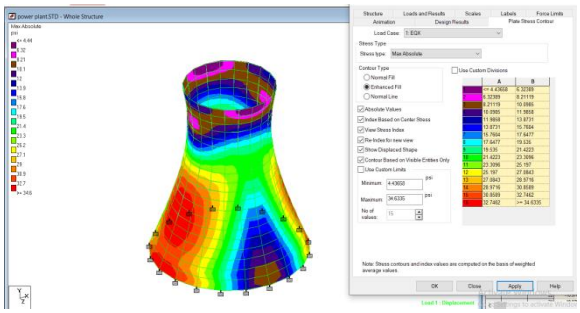

Figure1.7: Absolute stresses due to earthquake load

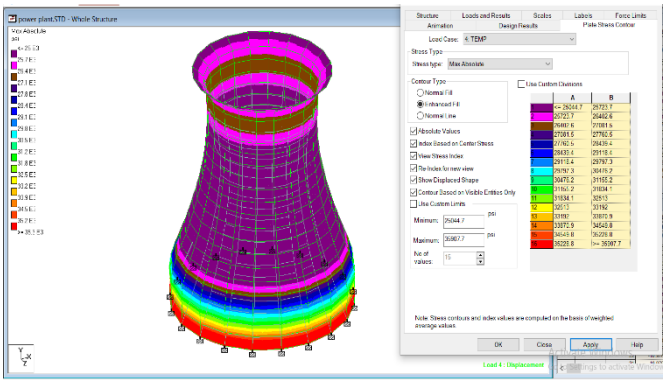

Figure1.8: Absolute stresses due to temp load

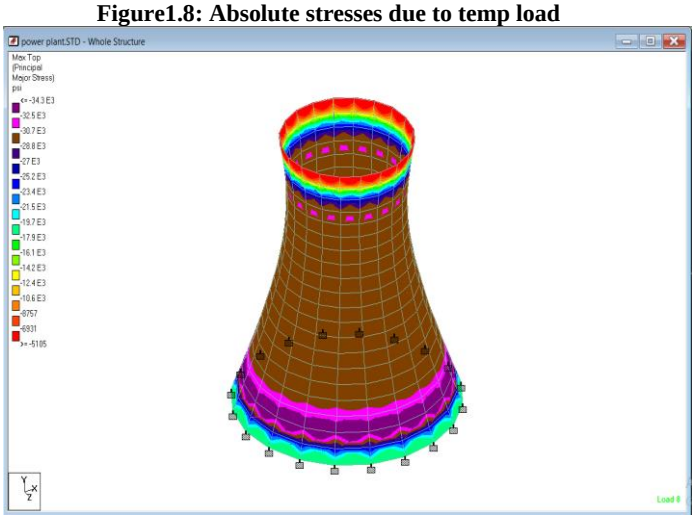

Figure1.9: Major Principal stresses at top

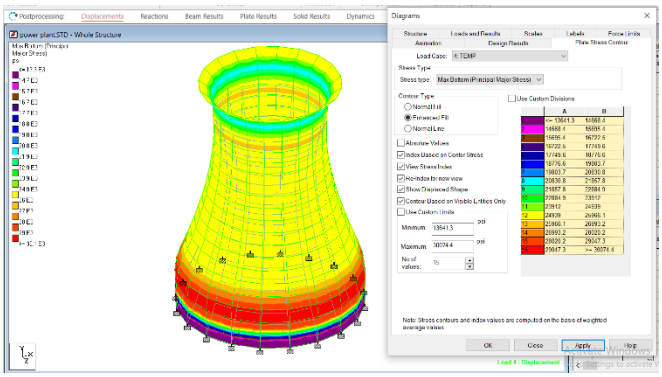

Figure1.10: Max bottom principal stresses due to temp effect

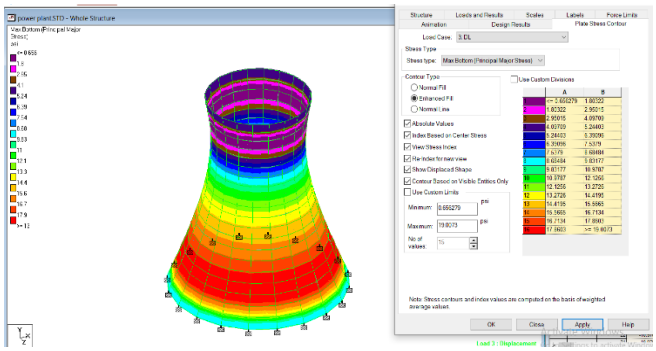

Figure1.11: Max bottom principal stresses due to dead load

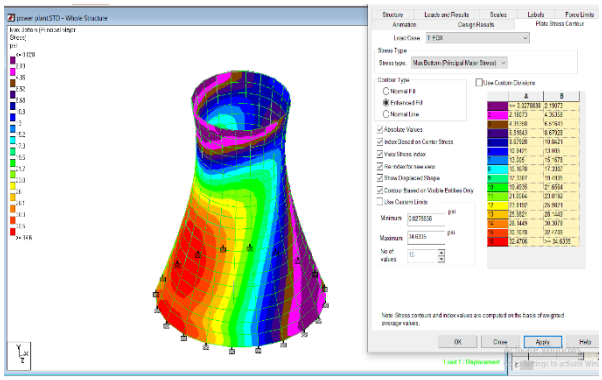

Figure1.12: Max bottom principal stresses due to earthquake load

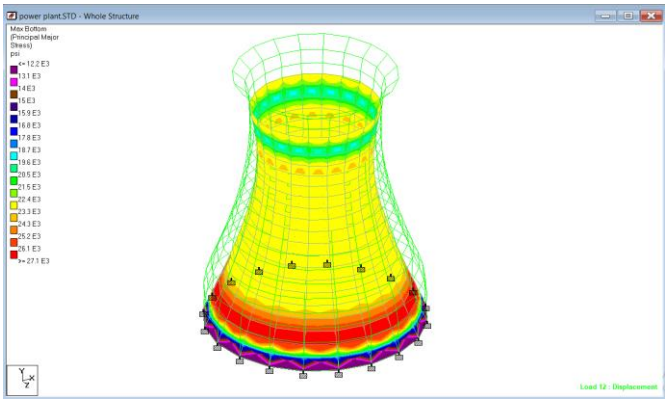

Figure1.15: Maximum principal stresses at bottom

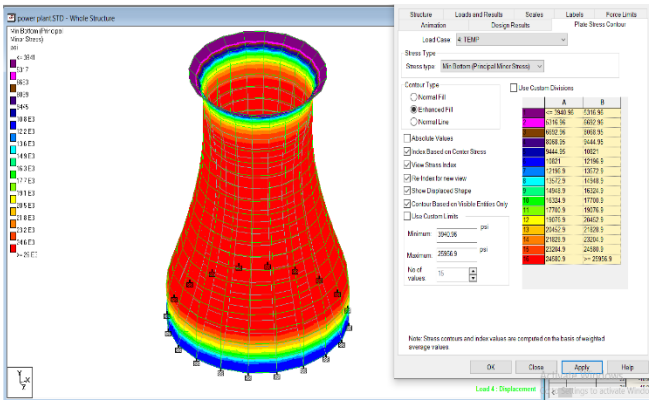

Figure1.16: Min bottom principal stresses due to temp effect

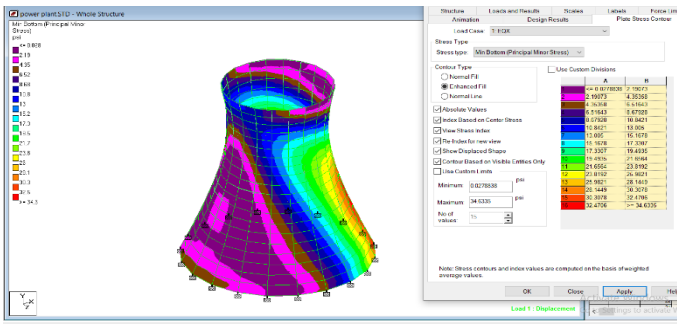

Figure1.18: Min bottom principal stresses due to earthquake load

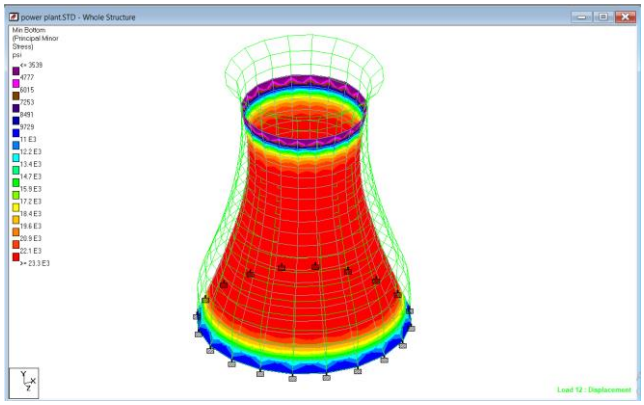

Figure1.21: Minimum principal stresses at bottom

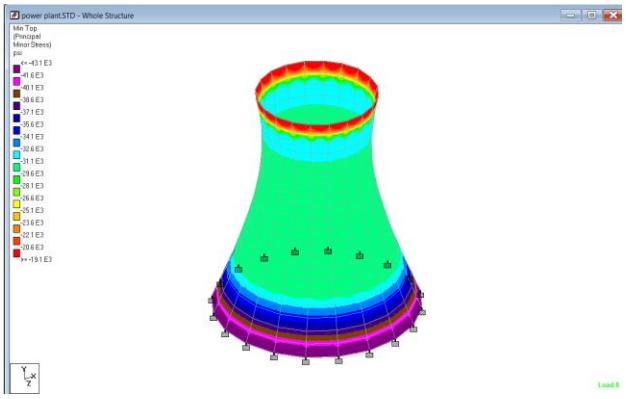

Figure1.22: Minor principal stresses at top

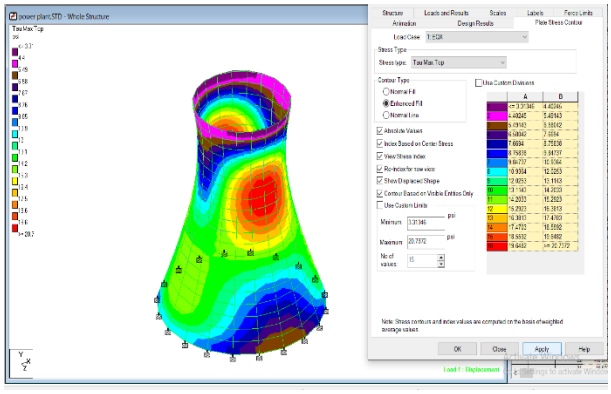

Figure1.23: Tau max at top stresses due to earthquake load

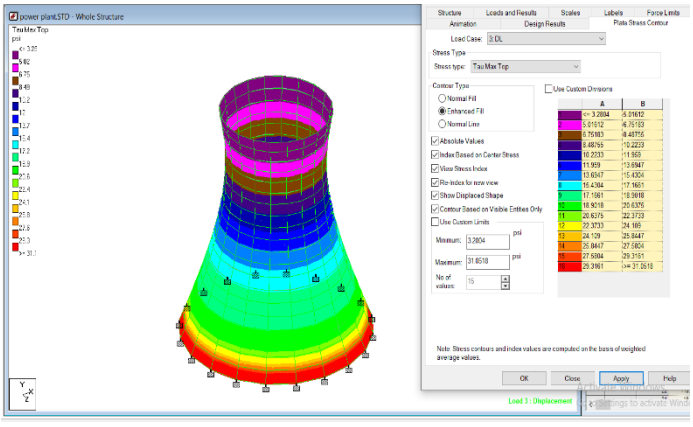

Figure1.25: Tau max principal stresses due to dead load

Table1.1: Displacement Due to Temperature Loading

			Horizontal	Vertical	Horizontal	Resultant	Rotational		
	Node	L/C	X in	Y in	Z in	in	rX rad	rY rad	rZ rad
Max X	6	3TEMP	2.409	4.962	0.000	5.516	0.000	-0.000	-0.045
Min X	16	3TEMP	-2.409	4962	-0.000	5.516	-0.000	-0.000	0.045
Max Y	24	3TEMP	0.846	5.112	0.615	5.218	0.006	0.000	-0.000
Min Y	5	4ULC, 1.5De	0.001	-0.020	0.000	0.020	0.000	0.000	-0.000
Max Z	1	3TEMP	-0.000	4.962	2.409	5.516	0.045	0.000	0.000
Min Z	11	3TEMP	0.000	4.962	-2.409	5.516	-0.045	-0.000	-0.000
Max rX	1	3TEMP	-0.000	4.962	2.409	5.516	0.045	-0.000	0.000
Min rX	11	3TEMP	0.000	4.962	-2.409	5.516	-0.045	-0.000	-0.000
Max rY	341	3TEMP	-0.000	1.546	1.722	2.314	0.005	0.000	0.000
Min rY	263	3TEMP	0.832	2.462	1.145	5.840	-0.000	-0.000	0.000
Max rZ	16	3TEMP	-2.409	4.962	-0.000	5.516	-0.000	-0.000	0.045
Min rZ	6	3TEMP	2.4.9	4.962	0.000	5.516	0.000	-0.000	-0.045
MaxRst	1	3TEMP	-0.000	4.962	2.409	5.516	0.045	-0.000	0.00

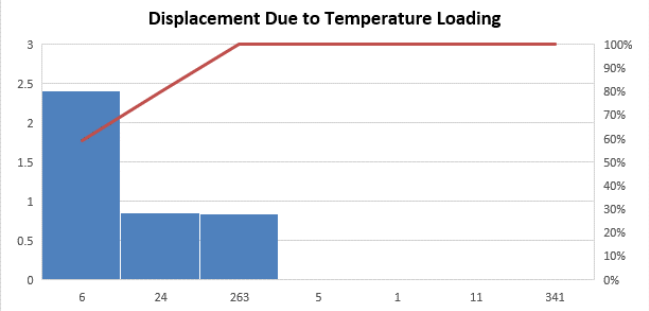

Graph 1.1Displacement Due to Temperature Loading

Table1.2: Maximum Base Reaction

			Horizontal	Vertical	Horizontal	Moment		
	Node	L/C	Fx kN	Fy kN	Fz kN	Mx Kip-in	My Kip-in	Mz Kin-in
Max Fx	416	3TEMP	29060.751	1.174	0.129	21.364	8.525	5851.142
Min Fx	406	3TEMP	29060.751	1.174	0.129	21.364	8.525	5851.142
Max Fy	405	4ULC,1.5De	435.481	1152.53	141.507	380.797	0.004	1171.888
Min Fy	405	3TEMP	27637.314	1.134	8980.224	1802.854	2.986	5562.602
Max Fz	411	3TEMP	0.129	1.174	29060.751	5851.142	8.525	21.364
Min Fz	401	3TEMP	0.129	1.174	29060.751	5851.142	8.525	21.364
Max Mx	401	3TEMP	0.129	1.174	29060.751	5851.142	8.525	21.364
Min Mx	411	3TEMP	0.129	1.174	29060.751	5851.142	8.525	21.364
Max My	401	3TEMP	0.129	1.174	29060.751	851.142	8.525	21.364
Min My	402	3TEMP	8980.455	0.812	27638.259	5557.927	8.070	1827.598
Max Mz	416	3TEMP	29060.751	1.174	0.129	21.364	8.525	5851.142
Min Mz	406	3TEMP	29060.751	1.174	0.129	1.364	8.525	5851.142

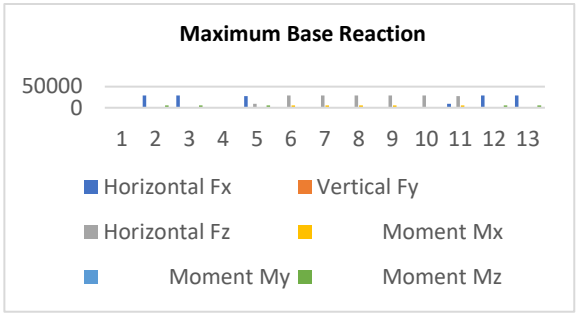

Graph1.2: Maximum Base Reaction

Table1.3: Shear Force and BMD Result

			Shear		Membrane			Bending Moment		
	Plate	L/C	SQX(Local) Psi	SQY(Local) psi	SX(Local)	SY(Local) psi	SXY(Local) psi	Mx Ib-in/in	My Ib-in/in	Mxy Ib-in/in
MaxQx	1	3TEMP	0.009	690.871	4902.833	157.304	-0.010	1.343	264.6	1.567
MinQx	5	3TEMP	0.019	690.871	4902.840	157.290	0.012	1.343	264.6	1.782
MaxQy	384	3TEMP	0.003	1422.644	1243.592	612.179	0.028	1.515	920.5	1.511
MinQy	22	3TEMP	0.002	740.281	2671.974	126.926	-0.004	1.525	1.111	0.704
MaxSx	2	3TEMP	0.001	690.874	4902.842	157.292	0.004	1.343	264.6	0.469
MinSx	381	3TEMP	0.008	1422.637	12438.70	612.717	0.042	1.515	920.5	0.750
MaxSy	324	3TEMP	0.001	155.213	374.810	62.908	0.011	1.652	1.790	0.838
MinSy	381	3TEMP	0.008	1422.637	12438.70	612.717	0.042	1.515	920.5	0.750
Max	362	3TE	0.001	373.748	6521.13	154.17	0.049	1.68	1.	0.674
Sx		MP							83	
MinSxy	325	3TEMP	0.004	155.128	374.763	62.884	0.056	1.652	1.790	0.061
MaxMx	351	4ULC, 1.5De	0.000	-0.185	26.111	90.690	0.000	98.62	375.9	0.008
MinMx	344	3TEMP	0.002	88.117	1662.256	38.702	0.016	1.689	1.939	1.173
MaxMy	341	4ULC, 1.5De	0.000	0.185	26.11	90.690	0.000	98.62	375.9	0.008
MinMy	344	3TEMP	0.002	88.117	1662.256	38.702	0.016	1.689	1.939	1.173
MaxMxy	365	3TEMP	0.006	373.741	6521.119	154.170	0.025	1.683	1.831	1.942
MinMxy	5	3TEMP	0.010	690.871	4902.840	157.170	0.012	1.343	264.6	1782

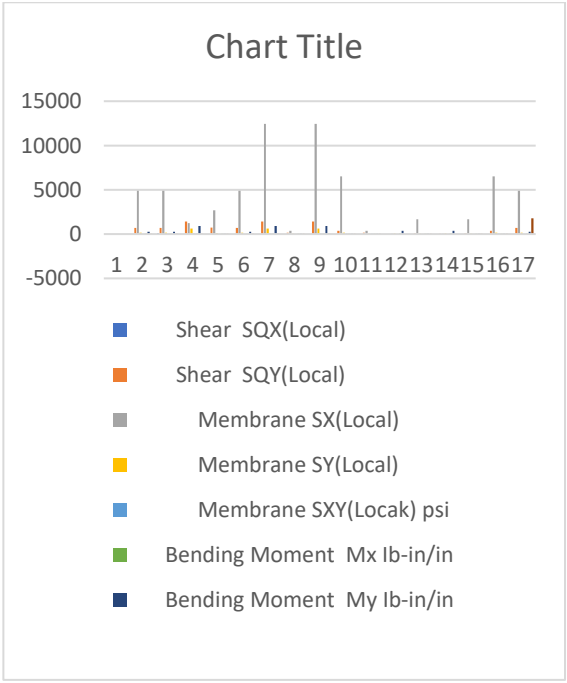

Graph1.3: Shear Force and BMD Result

Table1.4: Shear Force and BMD Result

			Shear		Membrane			Bending moment		
Plate	L/C	Node	SQX(Local) psi	SQY(Local) psi	SX(Local) Psi	SXY(Local) psi	SXY(Local) Psi	Mx Lb-in/in	My Lb-in/in	Mxy lb-in/in
1	2DL	1	0.001	0.122	7.515	2.184	0.261	43.359	176.721	14
		2	0.001	0.122	7.515	2.184	0.261	43.368	176.723	14
		22	0.001	0.121	3.797	2.483	0.220	21.140	72.069	15
		21	0.001	0.121	3.797	2483	0.220	21.136	72.069	15
	3TEMP	1	7.641	695.51	12760	2.483	766.10	126.76	307 41.1	89 86
		2	7.607	695.52	2760.7	288.36	766.05	126.40	307 40.4	89 86
		22	7.316	686.22	2843.2	559.60	598.77	1.41924	555.052	9471
		21	7.318	686.21	2843.1	559.53	598.77	1.41923	555.243	9472
	4ULC, 1.5De	1	0.002	0.183	11.272	3.277	0.391	65.038	265.082	21
		2	0.002	0.183	11.272	3277	0.391	65.052	265.085	21
		22	0.002	0.181	5.695	3.725	0.330	31.710	108.103	23
		21	0.002	0181	5.695	3.725	0.330	31.704	108.104	23
	5ULC, 1.2De	1	0.002	0.147	9.018	2621	0.131	52.031	212.066	17
		2	0.002	0.147	9.018	2621	0.131	52.042	212.068	17
		22	0.002	0.145	4.556	2980	0.264	25.368	86.482	18
		21	0.002	0.145	4.556	3.080	0.064	36.368	86.483	18

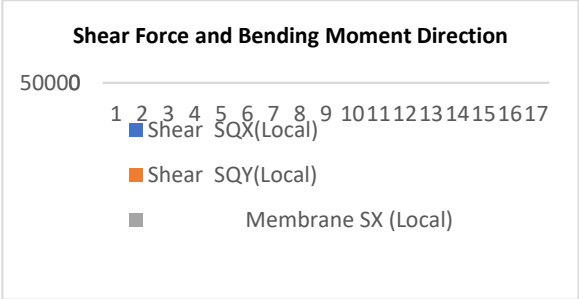

Graph1.4: Shear Force and BMD Result

Tables1.5: Absolute stresses due to earthquake load

Sr. No.	X-axis	Y- axis
1	4.43658	6.32
2	6.32389	8.21
3	8.21119	10.1
4	10.9858	12
5	11.9858	13.9
6	13.8731	15.8
7	15.7604	17.6
8	17.6477	19.5
9	19.535	31.4
10	21.4223	23.3
11	23.3096	25.2
12	25.197	27.1
13	27.0843	29
14	28.9716	30.9
15	30.8589	32.7
16	32.7462	34.6

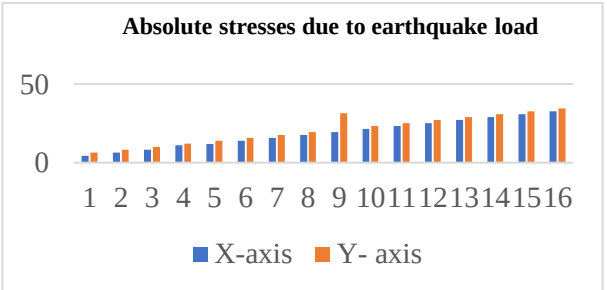

Graph1.5: Absolute stresses due to earthquake load

Table5.13: Min bottom principal stresses due to dead load

	X-Axis	Y-Axis
1	4.25808	8.01327
2	8.01327	11.7685
3	11.7685	15.5236
4	15.5236	19.2788
5	19.2788	23.034
6	23.034	26.7892
7	26.7892	30.5444
8	30.5444	34.2996
9	34.2996	38.0548
10	38.0548	41.81
11	41.81	45.5652
12	45.5652	49.3203
13	49.3203	53.0755
14	53.0755	56.8307
15	56.8307	60.5859
16	60.5859	64.3411

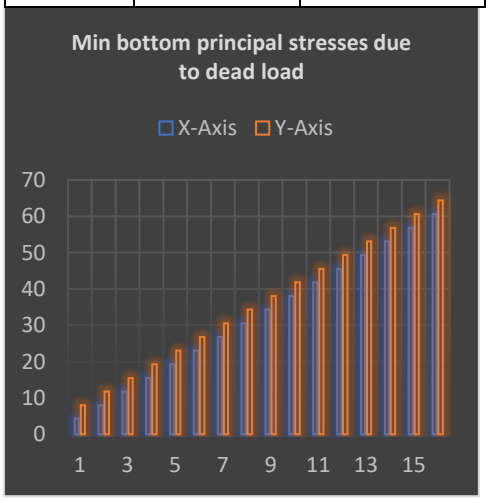

Graph5.13: Min bottom principal stresses due to dead load

	X-Axis	Y-Axis
1	0.419093	5.07216
2	5.07216	9.72523
3	9.72523	14.3783
4	14.3783	19.0314
5	19.0314	23.6844
6	23.6844	28.3375
7	28.3375	32.9906
8	32.9906	37.6436
9	37.6436	42.2967
10	42.2367	46.9498
11	46.9498	51.6029
12	51.6029	56.2559
13	56.2559	60.909
14	60.909	65.5621
15	65.5621	70.2151
16	70.2151	74.8682

Table5.14: Min bottom principal stresses due to earthquake load

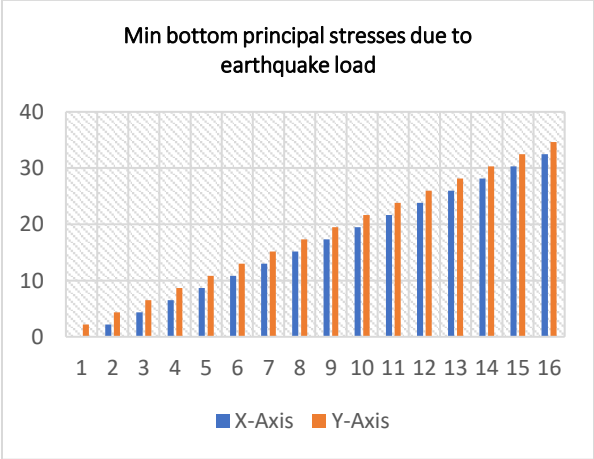

Graph5.14: Min bottom principal stresses due to earthquake load

	X-Axis	Y-Axis
1	0.0278838	2.19073
2	2.19073	4.35358
3	4.35358	6.51643
4	6.51643	8.67928
5	8.67928	10.8421
6	10.8421	13.005
7	13.005	15.1678
8	15.1678	17.3307
9	17.3307	19.4935
10	19.4935	21.6564
11	21.6564	23.8192
12	23.8192	25.9821
13	25.9821	28.1449
14	28.1449	30.3078
15	30.3078	32.4706
16	32.4706	34.6335

Table5.15: Min principal stresses due to dead load

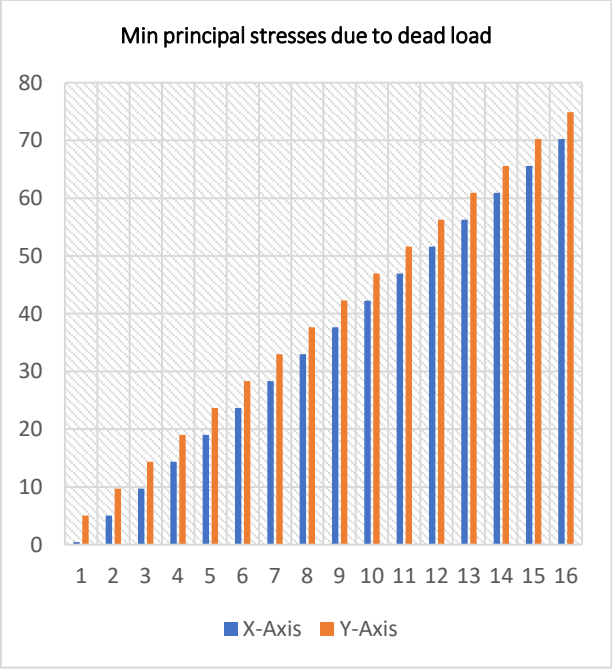

Graph5.15: Min principal stresses due to dead load

CONCLUSION

- In the equally tapered seismic investigation region, displacement graphs showed increased displacement at all heights. Thin structure displacements rise with height.
- Seismic and response spectrum analysis joint displacement decrease sequentially:
- Uniform taper to one-third of 84-meter chimney.
- Displacement will reach 84m chimney height. The 84m uniform tapering portion needs 130.76mm wind analysis displacement data.
- Maximum displacement effects require parametric design, unlike other models.
- To limit seismic and wind load displacement, the finest RC chimneys are tapered and taller.
- Maximum bending moment: 250.66 kilonewton meter DL+TEMP+EQX stress at bottom 30074.31 mpa.
- Maximum vertical reaction 29466.33 KN, bending moment 6817.58 Kip/in.

REFERENCES

[1]. Comparative Analysis of Structural Damage Potentials Observed in the 9.12 Gyeongju and 11.15 Pohang Earthquakes, Lee, Cheol-Ho, Kim, Sung-Yong, Park, Ji-Hun, Kim, Dong-Kwan, Elsevier, 19 April 2018

[2]. Improvement of Post-earthquake Risk Assessment System for Damaged Buildings by Case Study on '11.15 Earthquakes, Kang, Hyeong Gu, Yun, Nu-Ri, Kim, David, Lee, Jung Han, Elsevier 2018

[3]. Comparative Analysis of Earthquake Management in Pohang and Japan, Kim, Su Ran, Kim, Hye Won, Journal of Earthquake Engineering, 6 April 2019

[4]. Analysis of Reservoir Vulnerability Based on Geological Structure around Pohang Earthquake, Lim, Sung Keun, Song, Sung-Ho, Yu, Jaehyung, Science Direct 2018

[5]. Application Studies on Structural Modal Identification Toolsuite for Seismic Response of Shear Frame Structure, Chang, Minwoo, J Earthquake Eng Vol. 22 No. 3, 201-210, 2018

[6]. Prediction of Peak Ground Acceleration Generated from the 2017 Pohang Earthquake, Jee, Hyun Woo, Han, Sang Whang, Journal of Earthquake Engineering, 2019

[7]. Liquefaction Hazard Map Based on in Pohang Under Based on Earthquake Scenarios, Baek, Woo Hyun, Choi, Jae Soon, Ahn, Jae-Kwang, Elsevier 2018

[8]. Dynamic response analysis of intake tower in hydroelectric power station with high surrounding rock, Kangning Dang, Yunhe Liu, Jingyi Zhang, JVE International Ltd. Journal Of Vibro Engineering; MAY 2017

[9]. Earthquake and Wave Analysis of Circular Cylinder considering Water-Structure-Soil Interaction Piguang Wang , Yifu Chang, Mi Zhao , and Junyan Han, Research Article, 28 July 2020

[10]. Tuned mass damper system of high-rise intake towers optimized by improved harmony search algorithm H.Y. Zhang, L.J. Zhang, Journal of Engineering Structures

[11]. Application of dominant frequency for nonlinear dynamic analysis of embankment during an earthquake Behrouz

Gordan, Azlan Adnan, International Journal of Engineering and Advanced Research Technology (IJEART), 2018

[12]. Comparative analysis of dynamic characteristics of Intake Towers based on Pseudo-Static and Response Spectrum Method, L Z Huang, X Q Du, B H Huangfu and C Y Li, IOP Conference Series: Earth and Environmental Science, 2019

[13]. Probabilistic seismic response analysis of coastal highway bridges under scour and liquefaction conditions: does the hydrodynamic effect matter?, Xiaowei Wang, Advances in Bridge Engineering, 2020

[14]. Simulation analysis for the ultimate behavior of full-scale lead-rubber seismic isolation bearings M. Kikuchi, I. D. Aiken, Earthquake Engineering 2019

[15]. Shaking Table Test and Numerical Simulation On Seismic Behavior of a Receiver Tower in Concentrated Solar Power Plant Under Vertical Earthquake, Guoliang Bai, Bin Hao, October 25th, 2021

[16]. Seismic Behavior of Domestic Piloti-type Buildings Damaged by Pohang Earthquake, Kim, Taewan, Chu, Yurim, Journal of earth & Environment Engineering, 2017

[17]. Seismic performance of a separated selective-intake tower against level 2 seismic motions Koji Hino, Mikio NONAKA, Ryoichi FUJITA, 13th World Conference on Earthquake Engineering, 2018

[18]. Seismic Response Analysis of Nuclear Power Plant Structures and Equipment due to the Pohang Earthquake, Eem, Seung-Hyun, Journal of Earthquake Engineering, 2020

[19]. Application of Hydrodynamic Pressure for Three-dimensional Earthquake Safety Analysis of Dam Intake Towers, Bea, Jungju, Lee, Jeeho,

[20]. Seismic Performance of Steel Industrial Storage Racks Subjected to Korea Earthquakes, Jeon, Jong-Su, Choi, Hyoungsuk, Seo, Youngdeuk, Earthquake Engineering 2020

[21]. Instrumentation and control systems design for nuclear power plant: An interview study with industry practitioners Pooja Singh a, Lalit Kumar Singh, Nuclear Engineering and Technology, 2021

[22]. Design of safety critical and control systems of Nuclear Power Plants using Petri nets Pooja Singh a, Lalit Kumar Singh, Nuclear Engineering and Technology, 2019

[23]. Increasing the efficiency of nuclear power plant equipment at the design stage Mikle Egorov, E3S Web of Conferences 178, (2020)